21st Australasian Fluid Mechanics Conference
Adelaide, Australia
10-13 December 2018

Control of wall shear flows and the potential for "designer turbulence"

B. J. McKeon

Graduate Aerospace Laboratories
California Institute of Technology, Pasadena, CA 91125, U.S.A.

Abstract

This talk and paper draw heavily on related published work by this author reviewing flow control and especially the use of resolvent analysis to characterize and design control approaches. In particular, a range of almost identical material was presented at the 12^{th} International ERCOFTAC Symposium on Engineering Turbulence Modelling and Measurements [21].

The financial and environmental cost of turbulence is staggering: manage to quell turbulence in the thin boundary layers on the surface of a commercial airliner and you could almost halve the total aerodynamic drag on existing platforms, dramatically cutting fuel burn, emissions and cost of operation, and enabling new aircraft designs. Consequently, there have been large investments around the world in research into means to reduce and control turbulence [6]. However practical implementation, especially of active control schemes, has remained either impractical or not economically viable given relatively small net gains. A brief review of historical and current flow control efforts targeting skin friction reduction is given.

Systems-level tools to model scale interactions and control turbulence are given more detailed treatment. The resolvent analysis for turbulent flow proposed by McKeon and Sharma (J. Fluid Mech, 2010) [23] provides a simple, but rigorous, approach by which to deconstruct the full turbulence field into a linear combination of modes which interact through the nonlinear term to provide self-sustaining turbulence. A review of analysis of the linear resolvent operator and the nonlinear feedback, or the inter-connection between different scales which provides the forcing required for self-sustaining turbulence, is provided, then the formulation is extended to include control through modifications to the wall boundary conditions. After considering the information given by the resolvent operator about the relative physical locations of input and corresponding response, framed in the context of flow control, the specific examples of experimental manipulation of both the linear response and the triadic scale interactions using dynamic roughness actuation, opposition control and compliant wall design for global drag reduction are considered. A brief statement on the outlook for modeling and control of turbulent flows using this approach is also presented, focusing on possibilities related to a more general shaping of flow properties, or "designer turbulence", enabled by more detailed understanding of the mechanisms of turbulence sustenance.

Introduction to control of wall shear flows

Control of wall turbulence using passive or active means - as a sub-topic of the broader study of general flow control - has been a topic of scientific and especial practical interest for many years given the ubiquity of the phenomenon. Overviews of various approaches have been given by Gad-el-Hak [7], Kim [13, 14] and Kim and Bewley [15]. There have been various more recent efforts, as summarized by, e.g., McKeon, Jacobi and Duvvuri [22] as part of an AIAA Journal Special Issue on Flow Control. Henceforth in this contribution we focus specifically on the potential to use resolvent analysis for a system-level approach to flow control.

Closed Loop Resolvent Formulation

The resolvent formulation for wall turbulence has been described in detail in previous publications, e.g. [23, 24, 20]. The essential outline of the closed-loop resolvent analysis is shown in Figure 1, and the development here is for turbulent channel (plane Poiseuille) flow in a domain which is periodic in the streamwise and spanwise directions, x and z, respectively, with no-slip and no-penetration wall boundary conditions. Defining fluctuations relative to the spatio-temporal turbulent mean (which is assumed to be known from, e.g., experimental data, simulations or an eddy viscosity model), $\mathbf{U}(x,y,z,t) = \overline{U}(y) + \mathbf{u}(x,y,z,t)$, and Fourier transforming the Navier-Stokes equations in (x,z,t):

$$\hat{\mathbf{u}}(k_z, k_z, \omega; y) =$$
$$\int\int\int_{-\infty}^{\infty} \mathbf{u}(x,y,z,t) e^{-i(k_x x + k_z z - \omega t)} \mathrm{d}x\mathrm{d}z\mathrm{d}t$$

Rearranging, and formulating in velocity-vorticity form, (v, η), we arrive at

$$\begin{pmatrix} \hat{v} \\ \hat{\eta} \end{pmatrix} = \begin{pmatrix} \mathcal{H}_{vv} & 0 \\ \mathcal{H}_{\eta v} & \mathcal{H}_{\eta\eta} \end{pmatrix} \begin{pmatrix} \hat{g}_v \\ \hat{g}_\eta \end{pmatrix} \quad (1)$$

Here $\hat{g}_v$ and $\hat{g}_\eta$ represent a forcing of the linear terms at $\mathbf{k} = (k_x, k_z, \omega)$ arising from the nonlinear interactions between scales and the $\mathcal{H}$ operators constituting the resolvent (transfer function) are related to the well-known Orr-Sommerfield and Squire operators as follows, where $\kappa^2 = k_x^2 + k_z^2$, $\mathcal{D}^2$ is the Laplacian and U' is the local mean shear:

$$\mathcal{H}_{vv} = \left(-i\omega + (\kappa^2 - \mathcal{D}^2)^{-1} \mathcal{L}_{OS}\right)^{-1} \quad (2)$$
$$\mathcal{H}_{\eta\eta} = \left(-i\omega + \mathcal{L}_{SQ}\right)^{-1} \quad (3)$$
$$\mathcal{H}_{\eta v} = -ik_z \mathcal{H}_{\eta\eta} U' \mathcal{H}_{vv} \quad (4)$$

Input-output analysis of this form was described by Jovanovic and Bamieh [12] for laminar flow, and several other studies have considered the characteristics of the linear resolvent operator using an eddy viscosity rather than the explicit nonlinear term to provide a closure, e.g. Hwang and Cossu [10], or under a shaped stochastic forcing input, e.g. Zare, Jovanović and Georgiou [32].

Following the development of Rosenberg and McKeon [27], we further decompose the relationships above to reflect the potential independence of unforced Squire modes:

$$\begin{pmatrix} v \\ \eta \end{pmatrix} = \begin{pmatrix} v \\ \eta_{\text{os}} \end{pmatrix} + \begin{pmatrix} 0 \\ \eta_{\text{sq}} \end{pmatrix} \quad (5)$$

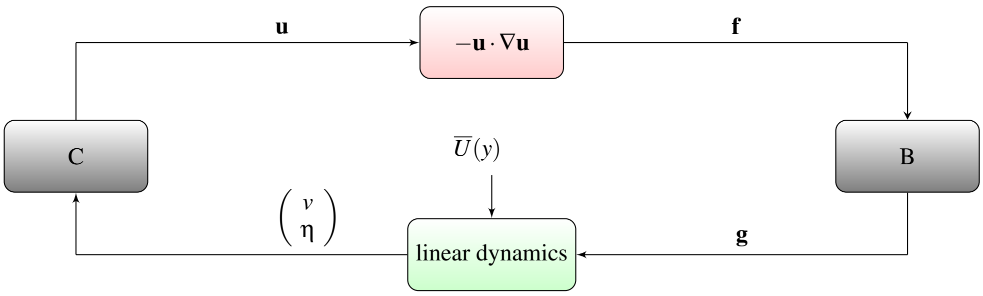

Figure 1: Schematic of the resolvent approach, after McKeon, Sharma & Jacobi [24].

with

$$\begin{pmatrix} v \\ \eta_{\text{os}} \end{pmatrix} = \begin{pmatrix} \mathcal{H}_{vv} & 0 \\ \mathcal{H}_{\eta v} & 0 \end{pmatrix} \begin{pmatrix} g_v \\ 0 \end{pmatrix} \tag{6}$$

$$\begin{pmatrix} 0 \\ \eta_{\text{SQ}} \end{pmatrix} = \begin{pmatrix} 0 & 0 \\ 0 & \mathcal{H}_{\eta\eta} \end{pmatrix} \begin{pmatrix} 0 \\ g_\eta \end{pmatrix} \tag{7}$$

Separate singular value decompositions (SVD) of the transfer functions for the Orr-Sommerfield and Squire modes can be used to obtain a set of forcing and associated response modes ranked by gain (respective singular values). The work of Rosenberg and McKeon outlines how this analysis is superior to the SVD of equation 1 in terms of providing a basis for reconstruction of the full turbulent field. The resolvent operator has been found to be surprisingly low-rank in the wavenumber-frequency range where turbulence is energetic (Moarref et al. [25]), such that only a low number of resolvent response modes are required to capture key physical features. The appropriate weights, $\chi_j(k_x, k_z, \omega)$, for each basis function can be determined either by consideration of the nonlinear interaction of response modes at other $\mathbf{k}$ combinations (McKeon, Sharma and Jacobi, [24]) or from data (Moarref et al, [25]; Gomez et al, [8]; Beneddine et al, [1]), allowing the full velocity field to be expressed as in equations 10-11. Thus this approach permits both the study of the most amplified response at each wavenumber pair and wavespeed ($c_{\mathbf{k}} = \omega/k_x$) and the importance of each nonlinear interaction.

Conceptually, open loop excitation can be viewed as adding an additional, external component to **f** in the schematic of Figure 1. The formulation can be modified to admit formal linear control, simply added here by implementing a wall boundary condition appropriate to the control law under consideration. These approaches have been advanced empirically and experimentally using dynamic roughness actuation at individual frequencies in a turbulent boundary layer (see, e.g., [24]) as well as more formally incorporating the true boundary condition change. Luhar, Sharma and McKeon [17] investigated opposition control (Choi, Moin and Kim, [2]) with a generalized (complex) amplitude, A_d, by implementing a wall-normal velocity at the wall of the opposite sign to the signal detected at an off-wall detection plane at height, y_d:

$$v_{\mathbf{k}}(0) + A_d v_{\mathbf{k}}(y_d) = 0 \tag{8}$$

A similar approach was used by Nakashima, Fukugata and Luhar [26], who investigated the effects of suboptimal control based on the shear stress measured on the wall, implementing wall transpiration proportional to the streamwise or spanwise wall shear stress.

Luhar, Sharma and McKeon [18] considered the interaction of simple compliant walls with turbulent channel flow. Consistent with earlier studies on compliant surfaces in the transitional flow regime, the dynamical wall boundary condition (for small deflections, constrained to be in the wall-normal direction only) was modeled using a complex admittance relating the wall-normal velocity and pressure at the wall,

$$Y = \frac{v_{\mathbf{k}}(0)}{p_{\mathbf{k}}(0)} \tag{9}$$

The analysis was subsequently expanded and developed as a potential design tool for compliant walls in Luhar, Sharma and McKeon [19].

$$\begin{pmatrix} v(k_x, k_z, \omega; y) \\ \eta_{\text{os}}(k_x, k_z, \omega; y) \end{pmatrix} \approx \sum_{j=1}^{N} \sigma_{\text{os}_j}(k_x, k_z, \omega) \chi_{\text{os}_j}(k_x, k_z, \omega) \psi_{\text{os}_j}(k_x, k_z, \omega; y) \tag{10}$$

$$\begin{pmatrix} 0 \\ \eta_{\text{SQ}}(k_x, k_z, \omega; y) \end{pmatrix} \approx \sum_{j=1}^{N} \sigma_{\text{SQ}_j}(k_x, k_z, \omega) \chi_{\text{SQ}_j}(k_x, k_z, \omega) \psi_{\text{SQ}_j}(k_x, k_z, \omega; y). \tag{11}$$

The studies outlined above all pertain to changes to the (boundary conditions on the) linear operator, but note that Luhar [16](2017) has also modeled the consequences of simple wall geometry changes on the nonlinear interactions in the resolvent framework.

Sensitivity to Forcing

With regards to physical insight into where actuation could influence a particular response mode, or the sensitivity of modes to forcing, Symon et al. [29] outlined the relationship between the locations of forcing and response in the resolvent for a range of different physical phenomena, as shown in the cartoon of Figure 2. For the turbulent channel flow, in which the mean profile, $\overline{U}(y)$, is one-dimensional, the Orr-type mechanism is active, with amplification arising due to both the mean shear (lift-up effect) and the presence of a critical layer, where $\overline{U}(y) = c_{\mathbf{k}}$. Both forcing and response are concentrated around the critical layer, with the former inclined upstream and the latter in the downstream direction. As shown in panels (i-l), a convective instability, as often associated with a two-dimensional mean flow leads to forcing and response modes with differing physical footprints: overlap of the modes reflects an effective wavemaker where actuation would be expected to be influential. Note that we do not formally address controllability and observability in this simple explanation.

Sharma et al [28] investigated direct excitation of the first forcing mode at individual $\mathbf{k}$ values using (off-wall) body forcing in a channel flow direct numerical simulation. Yeh & Taira [31] used resolvent analysis of uncontrolled separating flow over an airfoil to inform a frequency and spanwise wavelength for effective actuation using open-loop thermal actuation at the wall. Most practical actuation schemes are likely to be implemented at the wall and we detail next some results from schemes in which control has been applied to wall turbulence via the resolvent analysis.

Some Examples of Flow Control via Resolvent Analysis

Experiments using dynamic roughness actuation

Building on the results of Jacobi and McKeon [11], Duvvuri and McKeon [3, 4] utilized a spatially-impulsive oscillating spanwise strip - a dynamic roughness element - to provide external excitation at individual frequencies to a zero pressure gradient turbulent boundary layer, configuration which can be analyzed using the resolvent framework. The linear response of the flow was determined by phase-averaging downstream hot-wire and particle image velocimetry measurements with respect to the phase of the dynamic roughness. It was determined that the response, which decayed in the downstream direction, was dominated by a single streamwise wavelength for each frequency. Figure 3, from [3], shows the experimental configuration and summarizes the linear and nonlinear responses observed for a two frequency input, i.e. forcing at $\mathbf{k}_1 = (k_{x1}, 0, \omega_1)$ and $\mathbf{k}_2 = (k_{x2}, 0, \omega_2)$ which was shown to identify the sum and difference frequencies via the quadratic nonlinear interactions of the excited synthetic modes.

An extended summary of the results of these studies is given in [22]. In ongoing work (Huynh and McKeon, [9]), we are investigating the response of a compliant wall downstream of a dynamic roughness element using the framework of Luhar, Sharma and McKeon [18].

Opposition control in DNS

The generalized opposition control described by equation 8 was implemented on a scale-by-scale basis in turbulent pipe flow by Luhar, Sharma and McKeon [17]. For modes with a footprint in v at the detection plane, for example for the mode most closely corresponding to the near-wall cycle of turbulence (Figure 4), control modified both the response velocity field and the singular value (gain). Maximal gain reduction was obtained for different phases of control amplitude, A_d, for modes with different wavespeeds, $c_{\mathbf{k}}$. This behavior was captured by sweeps over $\mathbf{k}$ for the first response modes, i.e. a rank-1 approximation of the resolvent. Using the FIK identity (Fukugata, Iwamoto and Kasagi, [5]) to characterize the reduction in turbulent Reynolds stress (a proxy for the true drag reduction which includes a contribution from the laminar base flow) for traditional opposition control, $A_d = 1$, it was shown that the variation of the drag reduction trends with detection plane location were captured by the resolvent analysis. Further, an optimal drag reduction significantly larger than for the traditional parameters could be observed for control with $|A_d| = 1$ and $\angle A_d \approx \pi/4$.

Note that these results were obtained employing the uncontrolled turbulent mean in the formulation of the resolvent. In ongoing work, we have compared the predictions of the rank-1 linear analysis detailed above with the output of DNS at matched conditions, i.e. the full nonlinear solution (Toedtli, Luhar and McKeon, [30]). Not only are the trends in drag reduction matched across detection plane and actuation phase, but there is surprisingly good agreement between the conditions for optimal drag reduction. The sweep through this parameter space using the resolvent approach can be performed using desktop computing power rather than high performance computing capabilities, close to two orders of magnitude faster than for the DNS for this one-dimensional base flow. Further, the approach can be applied to Reynolds numbers beyond the capability of current DNS codes, however the gains decrease as the complexity of the base flow increases, e.g. through a two-dimensional base flow. Nonetheless, these results point to the potential to use resolvent analysis as a design tool to evaluate the likely efficacy of flow control techniques and the physics underlying them before devoting large computational resources at a particular control point.

Conclusions and Outlook

This paper has provided a brief introduction to current efforts to control wall turbulence. Some implementations of the full resolvent analysis framework in the context of flow control have been introduced. The approach configured for a no-slip and no-penetration wall boundary condition can be easily modified to account for various linear control laws. Examples of (spatially impulsive) dynamic roughness actuation of single frequencies and triadic interactions, and optimized opposition control have been briefly summarized.

The results described herein were generated using desktop computing power and Matlab ©, i.e. without resort to high performance computing. The approach provides a means of developing insight into the physics underlying unperturbed flows and mechanisms of self-sustenance of turbulent flows in general. The discussion here has focused on wall turbulence, but the technique is now being widely applied to a range of different flow configurations. In the context of flow control, the approach appears to have the potential to be used effectively as a design tool for evaluating and optimizing control schemes, as well as investigating questions related to practical implementation, for example the effects of limited spatial and temporal resolution (by restricting the range of $\mathbf{k}$ to which control can be applied), and sensing constrained to the wall. Combined with insight obtained from resolvent analysis with regards to the mechanisms of turbulence self-sustenance, it is proposed that there is an opportunity to use this tool to create "designer turbulence", or to shape the global properties of a flow in a systematic way.

Acknowledgements

The research described in this paper has been supported over many years by the U.S. Air Force Office of Scientific Research. Current support under grants FA 9550-16-1-0361 (AFOSR) and N00014-17-1-3022 (ONR) is gratefully acknowledged.

References

[1] Beneddine, S., Sipp, D., Arnault, A., Dandois, J. and Lesshafft, L., Conditions for validity of mean flow stability analysis and application to the determination of coherent structures in a turbulent backward facing step flow, *J. Fluid Mech.*, **798**, 2016, 485–504.

[2] Choi, H., Moin, P. and Kim, J., Active turbulence control for drag reduction in wall-bounded flows, *J. Fluid Mech.*, **262**.

[3] Duvvuri, S. and McKeon, B. J., Non-linear interactions isolated through scale synthesis in experimental wall turbulence, *Phys. Rev. Fluids*, **1**, 2016, 032401(R).

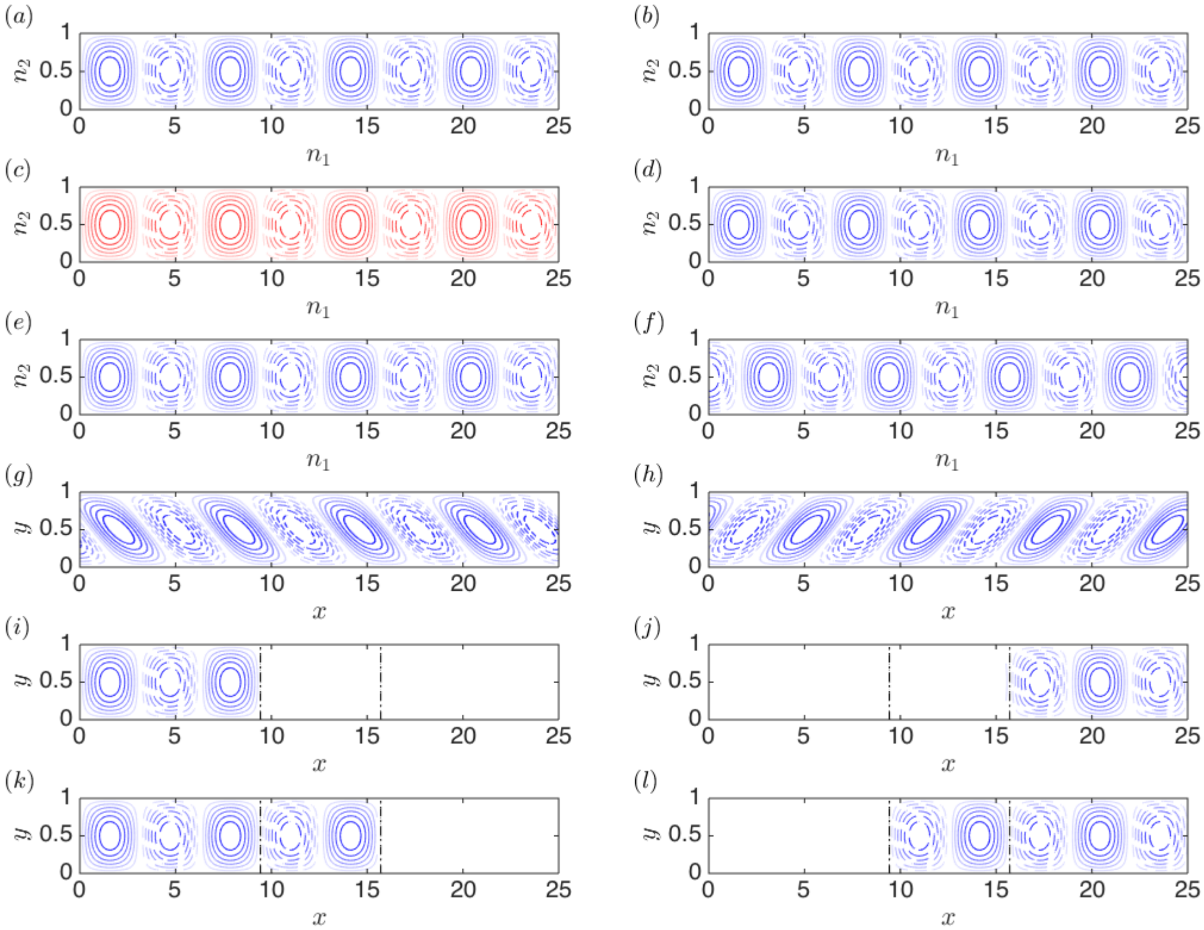

Figure 2: Schematic of forcing (left) and response (right) mode shapes for an example two-dimensional operator with amplification due to the following properties (from Symon et al, [29]). Panels (a, b) show resonant forcing and response, respectively, where the operator is self-adjoint (normal). (c, d) show component-type non-normality associated with the lift-up mechanism. (e, f): non-self-adjoint operator. (g, h): Orr-type mechanism. (i,j): convective-type instability. (k, l): convective instability with streamwise overlap between forcing and response modes (absolute instability) between vertical dashed lines. Positive (negative) isocontours are denoted by solid (dotted) lines and blue (red) indicates streamwise (transverse) components, in the x, y directions, respectively. Each mode is nonzero in one velocity component only.

[4] Duvvuri, S. and McKeon, B. J., Phase relations in a forced turbulent boundary layer: implications for modeling of high Reynolds number wall turbulence, *Phil. Trans. Royal Soc. A*, **375(2089)**.

[5] Fukugata, K., Iwamoto, K. and Kasagi, N., Contribution of Reynolds stress distribution to the skin friction in wall-bounded flow, *Phys. Fluids*, 73–76.

[6] Gad-el Hak, M., Interactive control of turbulent boundary layers: A futuristic overview, *AIAA Journal*, **32**.

[7] Gad-el Hak, M., *Flow Control: Passive, active and reactive flow management*, Cambridge University Press, 2000.

[8] Gómez Carrasco, F., Blackburn, H., Rudman, M., Sharma, A. and McKeon, B., A reduced-order model of three-dimensional unsteady flow in a cavity based on the resolvent operator, *J. Fluid Mech.*, **798**, 2016, R2.

[9] Huynh, D. and McKeon, B. J., Measurements of a forced, turbulent boundary layer over an elastic surface, *Bulletin of the APS*.

[10] Hwang, Y. and Cossu, C., Linear non-normal energy amplification of harmonic and stochastic forcing in the turbulent channel flow, *J. Fluid Mech.*, **664**, 2010, 51–73.

[11] Jacobi, I. and McKeon, B. J., Dynamic roughness-perturbation of a turbulent boundary layer, *J. Fluid Mech.*, **688**, 2011, 258–296.

[12] Jovanović, M. R. and Bamieh, B., Componentwise energy amplification in channel flows, *J. Fluid Mech.*, **534**, 2005, 145–183.

[13] Kim, J., Control of turbulent boundary layers, *Phys. Fluids*, **15**.

[14] Kim, J., Physics and control of wall turbulence, *Phil. Trans. Royal Soc. A*, **369**, 2011, 1396–1411.

[15] Kim, J. and Bewley, T. R., A linear systems approach to flow control, *Ann. Rev. Fluid Mech.*, 383–417.

[16] Luhar, M., Low-order models for turbulent flows over complex walls, in *Tenth International Symposium on Turbulence and Shear Flow Phenomena (TSFP-10), Chicago, IL*, 2017.

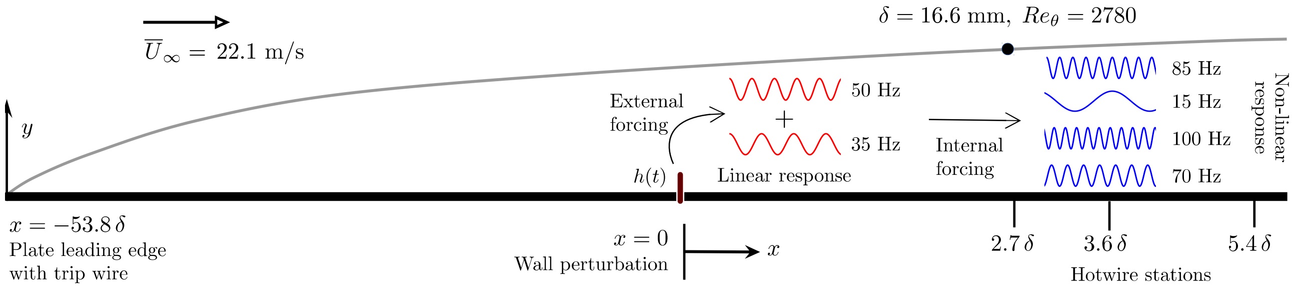

Figure 3: Schematic of dynamic roughness experiments, from Duvvuri and McKeon [3]. A spanwise element is oscillated at one or two frequencies to excite linear and nonlinear responses in a turbulent boundary layer, which are reconstructed by phase-locking downstream measurements to the phase of the dynamic roughness actuation.

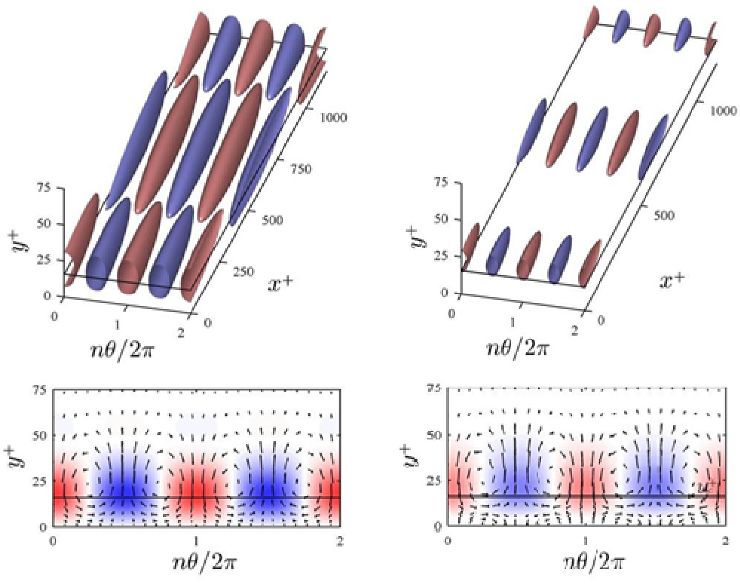

Figure 4: Isosurfaces of streamwise velocity (top) with cross-stream velocity vectors (bottom) for the first response mode with inner-scaled wavelengths and wavespeed $\lambda_x^+ = 1000$, $\lambda_z^+ = 100$ and $c^+ = 10$ in turbulent pipe flow at friction Reynolds number, $Re_\tau = 1100$. Left: uncontrolled flow. Right: under traditional opposition control, $A_d = 1$. Streamwise velocity isosurfaces are plotted at the same absolute level. The corresponding singular value for the controlled case is 0.6 times the uncontrolled value. Courtesy of M. Luhar.

[17] Luhar, M., Sharma, A. S. and McKeon, B. J., Opposition control within the resolvent analysis framework, *J. Fluid Mech.*, **749**, 2014, 597–626.

[18] Luhar, M., Sharma, A. S. and McKeon, B. J., A framework for studying the effect of compliant surfaces on wall turbulence, *J. Fluid Mech.*, **768**, 2015, 415–441.

[19] Luhar, M., Sharma, A. S. and McKeon, B. J., On the design of optimal compliant walls for turbulence control, *J. Turb.*, **17**, 2016, 787–806.

[20] McKeon, B. J., The engine behind (wall) turbulence: perspectives on scale interactions, *J. Fluid Mech.*, **817**, 2017, P1.

[21] McKeon, B. J., Modeling and control of wall turbulence via resolvent analysis, in 12^{th} *International ERCOFTAC Symposium on Engineering Turbulence Modelling and Measurements*, 2018.

[22] McKeon, B. J., Jacobi, I. and Duvvuri, S., Dynamic roughness for manipulation and control of turbulent boundary layers: An overview, *AIAA J.*, **56(6)**, 2018, 2178–2193.

[23] McKeon, B. J. and Sharma, A. S., A critical layer model for turbulent pipe flow, *J. Fluid Mech.*, **658**, 2010, 336–382.

[24] McKeon, B. J., Sharma, A. S. and Jacobi, I., Experimental manipulation of wall turbulence: a systems approach, *Phys. Fluids*, **25**.

[25] Moarref, R., Sharma, A. S., Tropp, J. A. and McKeon, B. J., Model-based scaling and prediction of the streamwise energy intensity in high-Reynolds number turbulent channels, *J. Fluid Mech.*, **734**, 2013, 275–316.

[26] Nakashima, S., Fukugata, K. and Luhar, M., Assessment of suboptimal control for turbulent skin friction reduction via resolvent analysis, *J. Fluid Mech.*, **828**, 2017, 496–526.

[27] Rosenberg, K. and McKeon, B. J., Efficient representation of exact coherent states of the Navier-Stokes equations using resolvent analysis, *Fluid Dyn. Res.*, **(to appear)**.

[28] Sharma, A., Moarref, R., Luhar, M., Goldstein, D. and McKeon, B. J., Effects of a gain-based optimal forcing on turbulent channel flow.

[29] Symon, S., Rosenberg, K., Dawson, S. T. M. and McKeon, B. J., Non-normality and classification of amplification mechanisms in stability and resolvent analysis, *Phys. Rev. Fluids*, **3**.

[30] Toedtli, S., Luhar, M. and McKeon, B. J., Comparison between dns data and resolvent model prediction of opposition control with a phase shift between sensor and actuator, *Bulletin of the APS*.

[31] Yeh, C.-A. and Taira, K., Resolvent-analysis-based design of airfoil separation control, *ArXiv 1805.02128*.

[32] Zare, A., Jovanović, M. R. and Georgiou, T. T., Color of turbulence, *J. Fluid Mech.*, **812**, 2017, 636–680.